

Laser-Fluorescence Ion-Beam Magnetic Resonance: Xe^+ Hyperfine Structure

S. D. Rosner, T. D. Gaily, and R. A. Holt

Department of Physics, University of Western Ontario, London, Ontario N6A 3K7, Canada

(Received 22 December 1977)

A new ion-beam magnetic resonance method using laser-induced fluorescence for both state selection and signal detection has been demonstrated for the first time. The hyperfine intervals of the $5d^4D_{7/2}$ level of $^{129}\text{Xe}^+$ and $^{131}\text{Xe}^+$ have been measured to better than 1 ppm accuracy.

Most of our knowledge of the structure of atomic and molecular ions has come from the optical spectra of discharge light sources; only in the last decade has there been significant progress in the application of rf spectroscopy techniques to ions. High-resolution magnetic resonance experiments have been carried out on ions in a cell, and in electromagnetic ion traps.¹ One technique that has not been generally applied to ions is the atomic-beam magnetic resonance (ABMR) method²; the reason is simply that large inhomogeneous magnetic fields are required for state selection. A notable exception was the pioneering measurement of the hfs of the $2^2S_{1/2}$ state in $^3\text{He}^+$ by Novick and Commins using a highly specialized method applicable to hydrogenic systems.³

The introduction of optical pumping as a replacement for the magnetic field state selector^{4,5} removes the fundamental difficulty in extending the ABMR technique to ion beams. In this Letter we report an rf magnetic resonance measurement of the hfs of the $5d^4D_{7/2}$ metastable level of $^{129}\text{Xe}^+$ and $^{131}\text{Xe}^+$ using laser-optimally-pumped beams of mass-separated isotopes. This follows an earlier measurement⁶ by laser optical spectroscopy on a Xe^+ beam. The present work, which improves the precision by a factor greater than 10^3 , represents the first demonstration of laser-fluorescence ion-beam magnetic resonance.

A schematic diagram of the apparatus is shown in Fig. 1. The 5-keV mass-selected ion beam is produced by a Colutron,⁷ which contains a hot-filament low-pressure dc arc source, a focusing lens, and a Wien-type mass filter. The space-charge-limited beam current density of $\approx 140 \text{ nA/cm}^2$ has an estimated metastable $5d^4D_{7/2}$ content

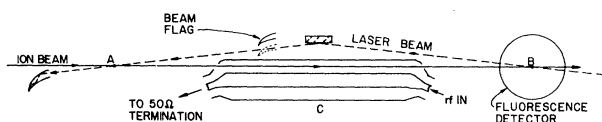


FIG. 1. Schematic diagram of the apparatus (not to scale); the z axis is normal to the plane of the drawing.

of roughly 0.1%. The ions intersect a single-mode cw dye-laser beam (region A), pass through an rf magnetic field (region C), and intersect the same laser beam again (region B). The laser-induced fluorescence at region B is detected by a cooled photomultiplier.

Figure 2 shows the hfs of the relevant levels of Xe^+ as derived from our earlier work.⁶ Since the Doppler absorption width of the beam is about 120 MHz (mainly due to the angular divergence of the ion beam), the laser can be tuned to excite a single hyperfine component, c for example. The excited ions decay primarily to the $6s^4P_{5/2}$ level (not shown) with the emission of fluorescence at 529.2 nm. The beam thus leaves region A with all the $F=4$ Zeeman sublevels almost entirely depopulated except for $M_F = \pm 4$. (We take the z axis along the linear polarization of the light.) If no resonant rf magnetic field is present in region C the populations remain unchanged, and the fluorescence at B is a small fraction of what it would be in an unpumped beam. When a field $H_1 \cos(\omega t) \hat{e}_z$ is tuned to the hyperfine transition frequency, ions are driven from $F=3$ to $F=4$ and the fluorescence at B increases.

The field H_1 is produced in a 50- Ω coaxial transmission line (see Fig. 1). This configuration was chosen to make the rf field very uniform over the 52.6-cm-long C region, and to minimize the mi-

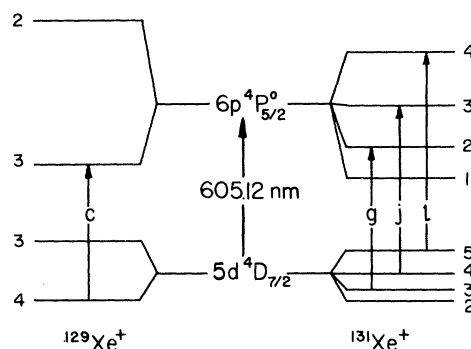


FIG. 2. Hyperfine structure in Xe^+ .

crowave power required. The rf frequency was counted, with a Sulzer-5D frequency standard as the reference. The ambient static magnetic field could be canceled to ± 3 mG by three sets of Helmholtz coils. The laser source has been described in Ref. 6. In this experiment one feedback loop was used to lock the laser frequency to an external temperature-stabilized Fabry-Perot etalon. The laser's intracavity mode-selecting etalon was then locked to the stabilized cavity mode with a second loop. Laser power at the *A* and *B* intersections was ≈ 40 mW in a 2-mm-diam spot. Typical fluorescence signals of 50 nA were obtained at a photomultiplier gain of $\approx 6 \times 10^6$, with an 18% quantum efficiency and a solid-angle efficiency factor for light collection of ≈ 0.2 .

The experimental procedure was as follows. With the laser beam blocked from reaching region *A*, the laser frequency was scanned over the 605.1-nm line as in Ref. 6. From the fluorescence pattern the mass separator could be sensitively adjusted to maximize the content of the desired isotope in the ion beam. Next, the laser was tuned to the correct hyperfine component and locked to the reference Fabry-Perot. The laser beam was allowed to intersect the ions at *A* and the consequent decrease in the fluorescence at *B* was maximized by varying the angle of intersection at *A* so that the Doppler shift was the same at both *A* and *B*.

Preliminary observations were made by scanning the rf frequency over the hyperfine resonance. A typical single scan at zero static field and an rf power of ≈ 0.8 W (approximately 20% of optimum) is shown in Fig. 3. The 150-kHz linewidth is due to the transit time of the ions in

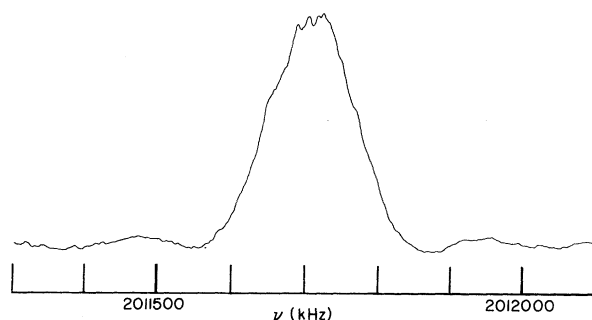


FIG. 3. X-Y recording of fluorescence at region *B* vs rf frequency. Vertical scale, arbitrary; frequency scale, approximate. Laser is tuned to optical transition *c*; rf is scanned over $F = 3 \leftrightarrow F = 4$ hfs transition. Time constant ≈ 0.4 sec. Static magnetic field is 0 ± 3 mG.

region *C*. The subsidiary maxima,² usually unobservable, are clearly evident as a result of the narrow ion velocity distribution. The line center was then determined by repeatedly setting the rf frequency to the half-amplitude points of the line profile, and the results are summarized in Table I. The observed frequencies must be corrected for the Doppler shift caused by the ion's velocity. The small errors in these corrections arise from uncertainties in the measurement of the accelerating voltage and plasma effects in the ion source. In a higher-precision experiment these Doppler corrections could be eliminated by taking data with the rf propagation direction reversed, and then averaging. The corrected frequencies in the last column of Table I were used to evaluate the hyperfine coupling constants for the $5d^4D_{7/2}$ level in the two isotopes using the formulas of Schwartz.⁸ The constants *A*, *B*, and *C* presented in Table II have not been corrected for perturbations⁹ from the $5d^4D_{5/2}$ level 41 cm^{-1} away. The need to include an octupole term is demonstrated by the large χ^2 obtained when *C* is set to zero.

This experimental method suffers from remarkably few systematic errors. For a slightly divergent ion beam, resonance line-shape asymmetry can arise with the simple crossing geometry used here because the optical Doppler shifts at *A* and *B* vary oppositely with drifts of the laser frequency or intersection angle. Ions which are not pumped at *A* can then contribute to the fluorescence at *B*, producing a spurious signal. Although this effect was averaged out in the present experiment, it could be eliminated by a fairly simple modification of the crossing geometry.

The possibility exists that the residual static field in region *C* could have distorted the line shape if the $\pm M_F$ components were not of equal

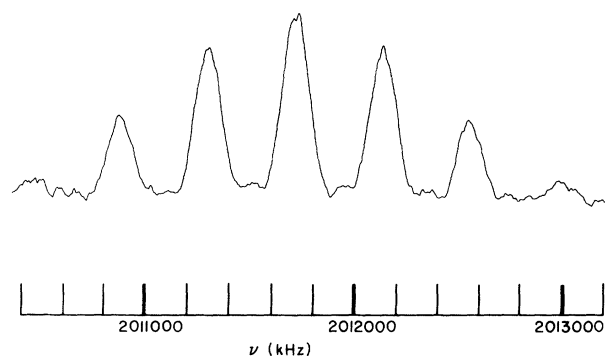


FIG. 4. Same as Fig. 3 with static field $859 \hat{e}_z$ mG along \hat{e}_z ; the vertical scale is expanded by $\frac{1}{3}$. The seven components are $M_F = -3$ to 3 .

TABLE I. hfs transition-frequency measurements in the $5d^4D_{7/2}$ level of Xe^+ . Errors are $\pm 2\sigma$.

Isotope	Transition ^a	ν_{measured} (kHz)	Doppler shift (kHz)	$\nu_{\text{corrected}}$ (kHz)
$^{131}\text{Xe}^+$	$4 \leftrightarrow 5$	$796\,357.0 \pm 1.2$	227.9 ± 0.2	$796\,584.9 \pm 1.2$
$^{131}\text{Xe}^+$	$3 \leftrightarrow 4$	$576\,109.5 \pm 1.0$	164.9 ± 0.1	$576\,274.4 \pm 1.0$
$^{131}\text{Xe}^+$	$2 \leftrightarrow 3$	$396\,591.2 \pm 1.2$	113.5 ± 0.1	$396\,704.7 \pm 1.2$
$^{129}\text{Xe}^+$	$3 \leftrightarrow 4$	$2011\,722.8 \pm 1.6$	580.3 ± 0.5	$2012\,303.1 \pm 1.7$
$^{129}\text{Xe}^+$	$3, 0 \leftrightarrow 4, 0$	$2011\,723.0 \pm 2.1$	580.3 ± 0.5	$2012\,303.3 \pm 2.2$

^aDenoted by $F \leftrightarrow F + 1$ for zero-field measurements and $F, M_F \leftrightarrow F + 1, M_F$ for the 859-mG measurement.

intensity. This was ruled out by splitting the line with a magnetic field of 859 mG in the z direction and showing that the center frequency of the $M_F = 0$ component was in excellent agreement with that of the zero-field line (see the last two rows of Table I and Fig. 4).

A significant narrowing of linewidth could be obtained by the use of the Ramsey separated oscillatory field technique²; however, for species that are long lived compared to the C -region time of flight (about $6 \mu\text{s}$ here), ions confined in cell buffer gases and especially in traps would still give narrower resonance lines. With the use of fast beams, the present technique should be well suited to the study of short-lived states and radioactive species. Signal-to-noise ratios can be very good, as in Figs. 3 and 4, which were obtained in a single sweep with no other processing than 0.4-s time constant. In a comparison of a similar measurement in a beam and in a trap,¹⁰ the trap gave narrower lines but a poorer signal-to-noise ratio. The case of Xe^+ is not the most favorable because of the low metastable content of the beam; on the other hand, the line strength of the optical pumping transition is large, and the technique is quite sensitive to this. It should be pointed out that optical resolution of the hyperfine or Zeeman splittings is by no means an essential part of this method; the M_F dependence of

the optical absorption produces the necessary alignment in the general case.⁵

A very important feature of the method is that in region C the ions are entirely free of the perturbing effects of the intense pumping light, collisions, and strong rf or static electromagnetic fields, so that most systematic frequency shifts encountered in cell and trap experiments are eliminated. The absence of collisions also makes it possible to study highly reactive species.

One of the attractions of the technique is its simplicity and flexibility: A completely identified beam of ions (or fast neutrals produced by charge exchange) can be studied in a specific state both optically and with rf to give signals of high quality. These features should be especially valuable in the study of molecular ions.

We gratefully acknowledge the technical assistance of I. Schmidt and J. Keyser, and the financial support of the National Research Council of Canada and the University of Western Ontario.

¹E. W. Weber, Phys. Rep. **32**, 123 (1977).

²N. F. Ramsey, *Molecular Beams* (Clarendon, Oxford, 1956), Chap. V.

³R. Novick and E. D. Commins, Phys. Rev. **111**, 822 (1958).

TABLE II. Effective hfs constants of the $5d^4D_{7/2}$ level of Xe^+ . Errors are $\pm 2\sigma$.

Isotope	A (kHz)	B (kHz)	C (kHz)	χ^2	DF ^a
$^{131}\text{Xe}^+$	149 156.40	71 107.0	0	7200	1
$^{131}\text{Xe}^+$	$149\,155.60 \pm 0.16$	$71\,110.1 \pm 1.1$	2.452 ± 0.059	...	0
$^{129}\text{Xe}^+$	$-503\,075.80 \pm 0.35$...	0

^aDegrees of freedom.

⁴J. Brossel, A. Kastler, and J. Winter, *J. Phys. Radium* **13**, 668 (1952).

⁵S. D. Rosner, R. A. Holt, and T. D. Gaily, *Phys. Rev. Lett.* **35**, 785 (1975).

⁶R. A. Holt, S. D. Rosner, and T. D. Gaily, *Phys. Rev. A* **15**, 2293 (1977).

⁷L. Wåhlin, *Nucl. Instrum. Methods* **27**, 55 (1964).

⁸C. Schwartz, *Phys. Rev.* **97**, 380 (1955).

⁹G. K. Woodgate, *Proc. Roy. Soc., Ser. A* **293**, 117 (1966).

¹⁰M. H. Prior and E. C. Wang, *Phys. Rev. A* **16**, 6 (1977).

E1-M1 Interference in Radiative Decay of Hydrogenlike Atoms in an Electric Field

Peter J. Mohr

Lawrence Berkeley Laboratory, University of California, Berkeley, California 94720

(Received 18 January 1978)

An unpolarized hydrogenlike atom in the metastable $2S_{1/2}$ state in an electric field decays primarily by one- or two-photon emission. The angular distribution of the single-photon radiation is expected to be asymmetric with respect to the electric field direction as a result of E1-M1 interference. Observable consequences of this effect in high- Z Lamb-shift experiments in progress are pointed out. A lowest-order estimate is given for the dependence of the asymmetry on the nuclear charge and the applied field strength.

Radiative decay of the $2S_{1/2}$ state in a static electric field has been studied in recent years as a means of determining the Lamb shift in hydrogen and hydrogenlike atoms. Both the lifetime of the excited state and the angular distribution of the emitted radiation, relative to the electric field direction, have been measured in order to infer values for the $2P_{1/2}$ - $2S_{1/2}$ energy splitting.¹⁻³

It is known that the angular distribution of electric-field-induced radiation from unpolarized hydrogenlike atoms is not isotropic, mainly because of the interference term between photon emission from the $2P_{1/2}$ and $2P_{3/2}$ states, which are mixed with the $2S_{1/2}$ state by the electric field. The anisotropy is characterized by a symmetric angular distribution of radiation of the form $a + b|\hat{k} \cdot \vec{E}|^2$, where \vec{E} is the electric field vector and \hat{k} is the direction of observation of the radiation. In high- Z hydrogenlike atoms, one may expect an additional asymmetric contribution (proportional to $\hat{k} \cdot \vec{E}$) to the angular distribution, which arises from interference between electric-field-induced electric dipole radiation and forbidden magnetic dipole radiation. For suitable combinations of nuclear charge and electric field strength, the ratio of the probability of photon emission in the direction of the electric field to the probability of emission in the opposite direction is less than 75%.

The purpose of this Letter is to point out the relevance of the asymmetry to high- Z Lamb-shift experiments now in progress, and give a lowest-order estimate of its magnitude. The asymmetry

can be expected to play a role in the analysis of experiments based on measurement of the anisotropy of electric-field-induced radiation from the $2S_{1/2}$ state.¹ In these experiments, the relative intensity of radiation in the directions parallel and perpendicular to the field direction is measured, and a value for the Lamb shift is inferred from the ratio. The asymmetric term gives field-strength-dependent contributions of opposite sign to the intensity in the directions parallel and antiparallel to the electric field. The asymmetry should also be taken into account in experiments based on measurement of the lifetime of the $2S_{1/2}$ state in an electric field by the time-of-flight method.² Here, because of magnetic field bending of the metastable atomic beam, single-photon decays are viewed at a varying angle with respect to the electric field direction, and the observed intensity is affected by the asymmetric as well as the symmetric contributions to the angular distribution. Under the conditions of either of these experiments, the asymmetry is a measurable effect.

One can readily verify that an asymmetric term in the transition rate is consistent with time-reversal invariance, even though \hat{k} changes sign under time reversal. An analogous situation arises, for example, in β decay where final-state Coulomb interactions give rise to terms which are proportional to combinations of polarization and momentum vectors, associated with the initial and final states, which are odd under time reversal while the interaction is assumed to be time-